CRREL REPORT 89-4

US Army Corps of Engineers
Cold Regions Research & Engineering Laboratory

(4)

Investigations of dielectric properties of some frozen materials using cross-borehole radiowave pulse transmissions

For conversion of SI metric units to U.S./British customary units of measurement consult ASTM Standard E380, Metric Practice Guide, *published by the American Society for Testing and Materials, 1916 Race St., Philadelphia, Pa. 19103.*

Cover: Array of boreholes (cased with PVC) in permafrost.

CRREL Report 89-4

March 1989

Investigations of dielectric properties of some frozen materials using cross-borehole radiowave pulse transmissions

Steven A. Arcone and Allan J. Delaney

Prepared for
OFFICE OF THE CHIEF OF ENGINEERS

UNCLASSIFIED

SECURITY CLASSIFICATION OF THIS PAGE

REPORT DOCUMENTATION PAGE

Form Approved
OMB NO. 0704-0188
Exp. Date: Jun 30, 1986

1a. REPORT SECURITY CLASSIFICATION Unclassified	1B. RESTRICTIVE MARKINGS
2a. SECURITY CLASSIFICATION AUTHORITY	3. DISTRIBUTION/AVAILABILITY OF REPORT Approved for public release; distribution is unlimited.
2b. DECLASSIFICATION/DOWNGRADING SCHEDULE	
4. PERFORMING ORGANIZATION REPORT NUMBER(S) CRREL Report 89-4	5. MONITORING ORGANIZATION REPORT NUMBER(S)
6a. NAME OF PERFORMING ORGANIZATION U.S. Army Cold Regions Research and Engineering Laboratory 6b. OFFICE SYMBOL (If applicable) CECRL	7a. NAME OF MONITORING ORGANIZATION Office of the Chief of Engineers
6c. ADDRESS (City, State, and ZIP Code) 72 Lyme Road Hanover, N.H. 03755-1290	7b. ADDRESS (City, State, and ZIP Code) Washington, D.C. 20314
8a. NAME OF FUNDING/SPONSORING ORGANIZATION 8b. OFFICE SYMBOL (If applicable)	9. PROCUREMENT INSTRUMENT IDENTIFICATION NUMBER
8c. ADDRESS (City, State, and ZIP Code)	10. SOURCE OF FUNDING NUMBERS PROGRAM ELEMENT NO. / PROJECT NO. 4A7627 30AT42 / TASK NO. D and SS / WORK UNIT ACCESSION NO. 005 and 014

11. TITLE (Include Security Classification)
Investigations of Dielectric Properties of Some Frozen Materials Using Cross-Borehole Radiowave Pulse Transmissions

12. PERSONAL AUTHOR(S)
Arcone, Steven A. amd Delaney, Allan J.

13a. TYPE OF REPORT	13b. TIME COVERED FROM ____ TO ____	14. DATE OF REPORT (Year, Month, Day)	15. PAGE COUNT
		March 1989	26

16. SUPPLEMENTARY NOTATION

17. COSATI CODES			18. SUBJECT TERMS (Continue on reverse if necessary and identify by block number)
FIELD	GROUP	SUB-GROUP	Alaska, Radiowaves, Dielectric properties, Site surveys, Frozen soils

19. ABSTRACT (Continue on reverse if necessary and identify by block number)

Pulsed radiowaves have been transmitted between boreholes at specially prepared sites in central Alaska to determine physical properties of the intervening material. The boreholes were drilled 12–25 m deep in both ice-rich silt and frozen alluvium, materials commonly found in the Alaskan interior. The pulse spectra were centered near 100 MHz and were analyzed to obtain the ground dielectric constant (ε) and the attenuation rate (β) which were then correlated with material type, water content and temperature. The ice-rich silt, which had volumetric ice contents between 47 and 70%, gave ε values between 4 and 7 and β values between 2 and 4 dB/m, thus limiting the use of our commercial equipment to borehole spacings of less than 20 m. For this material, ε correlated well with volumetric ice content but not with temperature. In a deep section (25 m), dielectric contrasts were seen between ice-rich silt, massive ice and frozen gravel. In the frozen alluvium, ε' values varied between 4 and 6 and β values were less than 1 dB/m, thus allowing signals to be received at a borehole spacing of over 40 m. Generally, ε' varied little with depth for any borehole pair. The pulses recorded at the widest spacings were due to direct transmissions and not to alternate, indirect paths that might include surface reflection or refraction. The observations thus demonstrate a method for reducing the number of boreholes commonly required for obtaining geotechnical information, and they provide data for determining borehole separation for a few common materials.

20. DISTRIBUTION/AVAILABILITY OF ABSTRACT	21. ABSTRACT SECURITY CLASSIFICATION
☒ UNCLASSIFIED/UNLIMITED ☐ SAME AS RPT. ☐ DTIC USERS	Unclassified
22a. NAME OF RESPONSIBLE INDIVIDUAL Steven A. Arcone	22b. TELEPHONE (Include Area Code) 603-646-4100 / 22c. OFFICE SYMBOL CECRL-RS

DD FORM 1473, 84 MAR

83 APR edition may be used until exhausted.
All other editions are obsolete.

SECURITY CLASSIFICATION OF THIS PAGE

UNCLASSIFIED

PREFACE

This report was prepared by Dr. Steven A. Arcone, Geophysicist, and Allan J. Delaney, Physical Science Technician, both of the Snow and Ice Branch, Research Division, U.S. Army Cold Regions Research and Engineering Laboratory. Funding for this research was provided by DA Project 4A762730AT42, *Design, Construction and Operations Technology for Cold Regions;* Task D, *Cold Regions Base Support: Design and Construction;* Work Unit 005, *Electromagnetic Methods for Rapid Subsurface Exploration;* and by DA Project 4A161102AT24, *Research in Snow, Ice and Frozen Ground;* Task SS, *Properties of Cold Regions Materials;* Work Unit 014, *Electromagnetic Characteristics of Snow, Ice and Frozen Ground.* This report was technically reviewed by Donald Albert and Dr. Kenneth Jezek of CRREL.

The contents of this report are not to be used for advertising or promotional purposes. Citation of brand names does not constitute an official endorsement or approval of the use of such commercial products.

CONTENTS

ILLUSTRATIONS

Figure

Page

Investigations of Dielectric Properties of Some Frozen Materials Using Cross-borehole Radiowave Pulse Transmissions

STEVEN A. ARCONE AND ALLAN J. DELANEY

INTRODUCTION

The use of geophysical measuring techniques for obtaining geological information in boreholes is a well-established practice. To date there are at least 17 electrical, seismic, chemical and nuclear techniques that can be applied to the rock wall of the borehole. In addition, vertical seismic profiling (VSP) and geophysical diffraction tomography (GDT) have been developed to expand the scope of investigation beyond the immediate vicinity of the borehole. GDT uses steady-state radiowaves propagated between boreholes to reconstruct, using Kirchhoff diffraction theory, the intervening distribution of electrical properties and thus to infer the geology. In this paper we discuss the use of pulsed VHF radiowaves propagated between boreholes to determine electrical and physical properties of frozen materials using simple ray optics.

The use of transients in the VHF or higher frequency range for geophysical surveying was first reported by Cook (1960) and Barringer (1965) and then realized in the 1970s in a commercially available system commonly known as "impulse" or ground-penetrating radar (e.g. Morey 1974). The system generally uses a bistatic antenna arrangement to allow better resolution of near-surface returns. This permitted the system to be applied to the WARR (wide-angle reflection and refraction) sounding technique (Annan and Davis 1976, Arcone 1984a), where antennas are continually separated to obtain propagation velocities associated with various events. Separated antennas have also been used for propagating pulses directly through geologic strata using tunnels (Arcone and Delaney 1984, Arcone 1984b). By the late 1970s, borehole antennas were commercially available, although very little (if any) information has been published on their use.

The objective of this research was to investigate the use of pulsed radiowaves as an expedient technique to measure ground dielectric properties between boreholes and thus to limit the drilling needed to characterize the material type of a planned construction site. Four or more boreholes between 12 and 25 m deep and spaced from 4 to 50 m apart were drilled at each of three sites near Fairbanks, Alaska. Two sites were located in ice-rich silt and the other was in frozen alluvium. Data were collected in the early spring and late summer from 1984 to 1986 using a commercially available subsurface radar that transmitted and received pulses with spectra centered near 100 MHz and lasting about 20 ns. Signal delay times and amplitudes were measured to calculate dielectric constants and attenuation rates, both of which were then correlated with volumetric and gravimetric ice content and temperature. The electrical investigations of the ice-rich silt at one site and the temperature and electrical resistivity data from two of the sites have been reported previously (Arcone and Delaney 1988, Delaney et al. 1988), and some of the material in this report can be found in these articles. The new material concerns the propagation data for frozen alluvium and for a second ice-rich silt site containing massive ice.

EQUIPMENT AND DATA PROCESSING

Electromagnetic equipment

A control unit manufactured by the Xadar Company (Electromagnetic Reflection Profiling System, model 1316) controlled a pair of borehole antennas (model H6/110) manufactured by the GSSI Company. The control unit is intended for profiling with the transmitting and receiving an-

tennas close together, but it may be used with the antennas at any separation. The pulse repetition frequency (PRF) was 50 kHz. The signals received within a fixed time interval are sequentially sampled to convert the VHF or UHF frequency content into the audio range for recording and playback. A more extensive description of this system can be found in Annan and Davis (1976) or Davis et al. (1976).

The control unit digitally records the received signals over one of several scan lengths, ranging from 43 to 2000 ns. The scans were linearly stacked to reduce incoherent noise and then stored on magnetic tape. An exponentially increasing gain was applied over the first quarter of the scan, after which it remained constant. An overall system gain was also used. Data were later transferred to a Hewlett Packard 9825 computer for playback and graphic display.

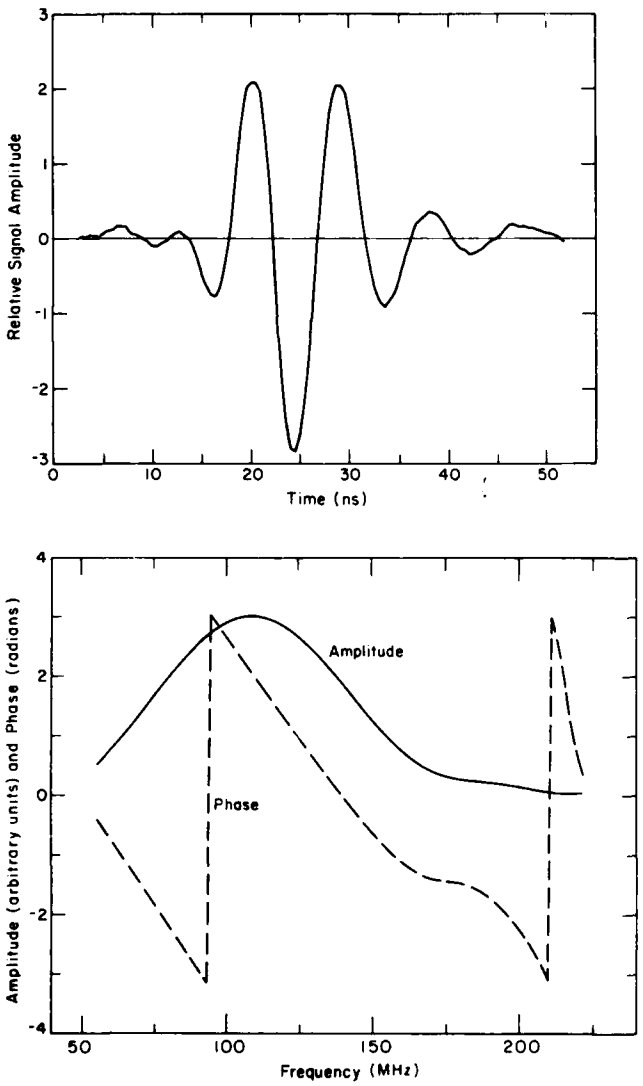

Figure 1. Typical transmitted wavelet (top) and its associated amplitude and phase spectra.

A typical radiated pulse shape and its associated Fourier spectrum are shown in Figure 1. Both the transmitting and receiving antennas are radially directional, although the pulse shape is maintained in all directions. Measurements made at the surface revealed that the received amplitude could vary as much as 2.6 dB, depending on the azimuthal orientation between the antennas. However, this could cause only a small adjustment in measured attenuation rates (in dB/m) when divided by the propagation distances. Antenna orientation in the boreholes was inhibited by the attached ropes and cables, but it was impossible to determine because the antennas would rotate to an equilibrium position when being lowered to the bottom of the hole.

The time delay was calibrated by recording pulse transmissions between antennas separated in air at measured distances. The absolute zero time reference for any borehole pair (i.e. two antennas lowered simultaneously) was determined by first measuring the time delay difference t_d between an air transmission over a distance equal to the borehole spacing, and a transmission between the boreholes (both recordings within 1 minute) at the maximum borehole depth. The borehole separation divided by the free space velocity (c = 30 cm/ns) was then added to t_d to locate the zero time reference. This procedure fixed the position of the absolute time reference on our recordings for all years of measurement. Temperatures recorded throughout the year at maximum borehole depths (12–25 m) revealed no seasonal changes, thus strengthening the assumption that there were no dielectric changes at those depths. In 1986, air calibrations for every borehole pair were taken within one minute of the bottom readings to compensate for drift in the zero time reference (approximately 1 ns/hour) because of changes in dc bias levels within the course of a day or between years, the latter of which could be as much as 14%. No adjustments in the zero time reference were made during any sequence of measurements between a particular borehole pair.

Signal amplitudes were calibrated using the gain settings and signal level recorded for each transmission. Signal attenuation rates between a borehole pair were deter-

mined by comparing the amplitudes received between that pair with those measured between a closer reference pair, for which total attenuation was generally less; 13 combinations of pairs were used. The rates are therefore based on relative measurements to eliminate system losses. Absolute calibrations were impossible because we did not know the initial signal strength at the antennas. Variations in received amplitude due to antenna impedance loading by the borehole walls were not considered, but they are thought not to be significant throughout any one sounding because of the uniformity of properties subsequently measured.

Resistivity

Strings of electrodes were mounted to 3.8-cm-diameter plastic (ABS) pipe and inserted down separate boreholes, one at each site, which were then backfilled with wet silt (at the silt sites) or sand and gravel (at the alluvium site) and allowed to refreeze. The electrodes were separated by 30 cm. DC resistivity was determined by comparing the voltage measured between a pair of adjacent electrodes to the current fed between their nearest neighbors in a Wenner-type array. An apparent resistivity ρ_a was computed using the formula for a Wenner array embedded in a *homogeneous earth:*

$$\rho_a = 4\pi a \frac{V}{I} \qquad (1)$$

where a = electrode spacing
V = voltage
I = current.

Figure 2 schematically illustrates the application of the Wenner array to the electrode string.

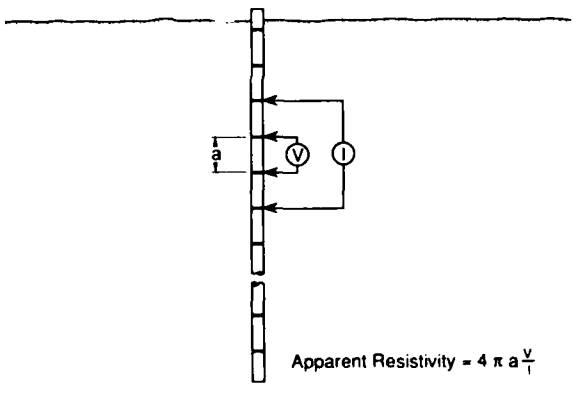

Figure 2. Borehole resistivity electrode string used in a moving Wenner array.

The quantity ρ_a is an apparent value that represents an integration over a radius of about $0.7a$, or about 20 cm; ρ_a equals the real resistivity only for homogeneous earth. A simplified, two-layer analysis showed that the air and plastic volume of the pipe could lower ρ_a by only a few percent. A more complete description of this experiment (including discussion of contact resistance) with data for 12 months is given by Delaney et al. (1988).

Temperature

Temperature T was measured every 30 cm using a thermistor probe slowly lowered down a separate borehole at each site filled with ethylene glycol. The calibration of the thermistor (Omega 400 series) worked out to approximately 40 ohms change per 0.1°C change in temperature. Resistance readings were stable to within ±4 ohms, thus giving an interpolated temperature reading accuracy of ±0.01°C. Readings were made on a battery-operated voltmeter after equilibrium was established at each level. The thermistor was weighted to facilitate lowering. An entire run lasted about 45 minutes.

Electromagnetic data reduction

The time delay and peak signal amplitude of each pulse transmission allowed computation of the complex index of refraction $n^* = n' - in''$ from which the complex dielectric permittivity $\varepsilon^* = \varepsilon' - i\varepsilon'' = n^{*2}$ could be calculated. The quantities n' and n'' are the real and imaginary parts of n, ε' and ε'' are the real and imaginary parts of ε^* and $i = \sqrt{-1}$. Time delays were measured at the leading edge of the wavelet and, with the known borehole separation, were used to determine n'. The position of the leading edge was determined visually to about 0.5 ns, which generally gives an error of less than 0.1 in ε'. The consistency in oscillation periods for all wavelets precluded the presence of dispersion and the possibility that *leading-edge velocities were not characteristic* of the main frequency components of the wavelets. Only the leading edge could be used because the wavelet length and spectrum in the air reference signals (centered at approximately 140 MHz) were different from those in the ground signals (100 MHz).

The attenuation rate β (dB/m) was computed by comparing the peak received signal strength A_2 for one pair with that for a closer, reference hole pair A_1. After adjusting the ratio A_2/A_1 for geometric spreading losses, β is then found from the formula

$$\beta = 20 \log (A_2/A_1)/\Delta Z \qquad (2)$$

where ΔZ is the difference in separation between the two borehole pairs. The imaginary part of the refractive index is then

$$n'' = \beta c / [8.68\,(2\pi f)] = 0.055\,\beta/f \qquad (3)$$

where f is the strongest frequency of transmission (in hundreds of MHz). The components of ε^* are then

$$\varepsilon' = n'^2 - n''^2 \qquad (4)$$

and

$$\varepsilon'' = 2n' n'' . \qquad (5)$$

The quantity n'' proved small enough to allow us to use $\varepsilon' = n'^2$ with an error within ±0.04, which is within the error of the time measurement.

Signal loss other than geometric spreading is caused by resistive or dipolar dispersional losses, or scattering. Delaney and Arcone (1984) have shown the dipolar component of ε'' to be in the range 0.1–0.2 for Fairbanks silt with a very high ice content, which at 100 MHz gives 0.4–0.8 dB/m for $\varepsilon' = 5$. Attenuation rates due to material resistivity ρ are computed from the formula

$$\beta_\rho = 4.34/c\sqrt{\varepsilon'}\;\varepsilon_0\rho = \frac{1636}{\rho\sqrt{\varepsilon'}} . \qquad (6)$$

where $\varepsilon_0 = 8.85 \times 10^{-12}$ Farad/m is the free space permittivity.

RESULTS AND DISCUSSION

Site 1: Ice-rich silt

This site is located at the Farmer's Loop Road test facility of CRREL in Fairbanks, Alaska. The soil type is retransported eolian silt that exists to a depth of several tens of meters at this site (Péwé 1958). Previous investigators (Arcone et al. 1978, Arcone and Delaney 1982, Sellmann et al. 1983) have reported values for ground resistivity and active-layer dielectric constant. Generally the volumetric ice content (discussed later) exceeds 50%, and the active layer depth is 70–100 cm. An organic mat covers the surface. The lowest and highest ground temperatures occur in early spring and late summer, respectively.

Six holes (Fig. 3) were drilled to approximately 12 m deep and cased with 3-in.-diameter (7.62-cm) ABS plastic pipe, capped and sealed at the

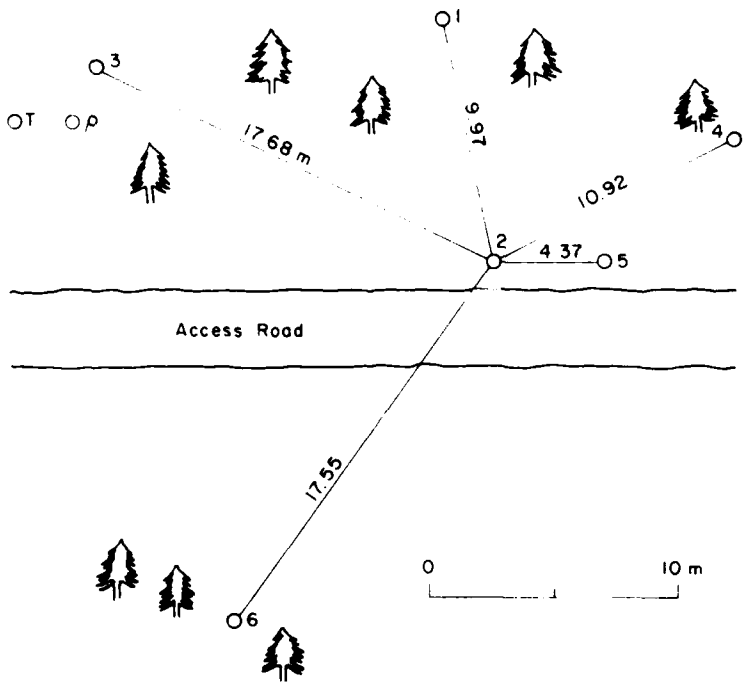

Figure 3. Borehole layout at Site 1, the Farmer's Loop Road test facility in Fairbanks, containing high-ice-content silt. T *and* ρ *are the temperature and resistivity electrode string boreholes.*

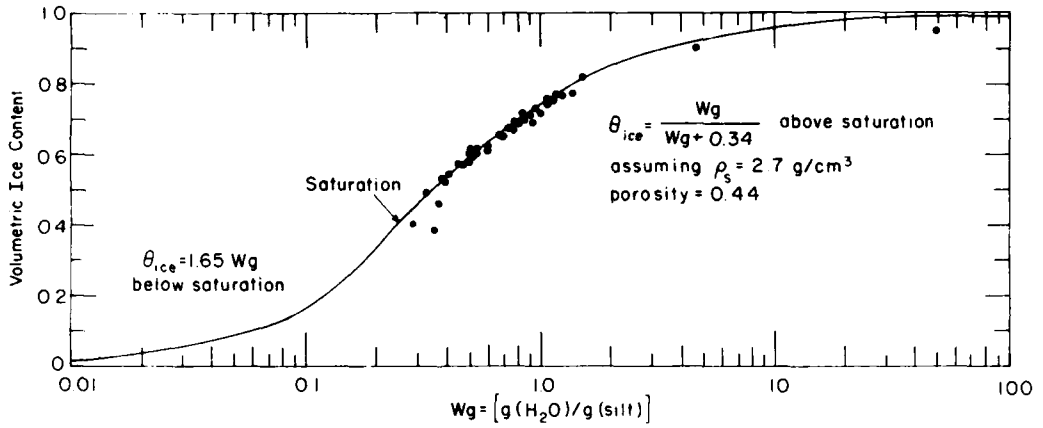

Figure 4. Calibration data and matching theoretical curves for determining volumetric ice content from gravimetric water content.

bottom. Core samples could not be obtained because freeze-back of the core barrel to the hole wall constantly occurred at the near-0°C temperature of the soil. Consequently only augered cuttings were obtained at regular depths from which the gravimetric water content was measured. Massive ice was not encountered in any of the holes.

Equivalent volumetric ice content was calculated using a calibration curve (Fig. 4) matched to data from cores obtained at a nearby site near Fox, Alaska, containing the same type of ice-rich retransported silt as mapped by Péwé (1958), and from other studies at Fox and Farmer's Loop (Arcone and Delaney 1982). The equations for the curves assumed a silt density of 2.7 g/cm^3, a porosity of 0.44 (Hoekstra and Delaney 1974) and that $\theta_{ice} + \theta_{silt} + \theta_{air} = 1$. The symbol θ stands for volumetric content. Above saturation, $\theta_{air} = 0$. The volumetric unfrozen water content was not measured in the cores nor considered in the theory. This causes an error of a few percent in the saturation calculations because several grams of unfrozen water can exist for every 100 g of silt (Tice et al. 1978) below –0.7°C, the highest temperature encountered in the boreholes.

Pulse transmissions were recorded at 1-m depth intervals. The antennas were raised simultaneously from a bottom datum plane established by surface leveling. Nine borehole pairs were investigated for ε'. Figure 5 shows a typical record. The two widest pairs (boreholes FL 2–6 and FL 2–3, Fig. 3) gave limited or no discernible signal above the noise level. Generally transmissions in the top 3 m between each pair were severely affected by the noise generated by the sequential sampling of nearby FM radio stations, as is evident in Figure 5. None of the interborehole paths crossed a third borehole, and rarely was an event secondary to the direct transmission observed for any pair but the closest. The correlations between propagation characteris-

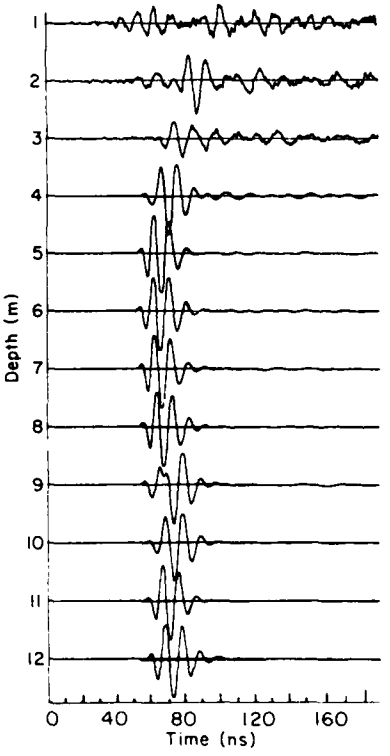

Figure 5. Example of interborehole pulse transmission record, in this case between holes FL4 and 5.

tics and ice content are treated statistically because no soil samples were obtained between boreholes.

Figure 6 shows the temperature and θ_{ice} profiles. The temperature profile was done on 4 April 1986, with an approximate snow cover of 30 cm and before any extensive thaw periods had begun. The temperature was constant below 6 m at –0.75°C. The volumetric ice content varied between 48 and 78%, and no formations of massive ice were found in any of the holes. The θ_{ice} profile for hole FL6 shows the largest fluctuations. This profile will not be included in subsequent averaging and comparisons, as the hole was too distant to receive any transmissions.

Figure 6 also compares 1985-86 average values of ε' with the averages for θ_{ice} for holes FL1–5. The lowest values of ε' correlate with the highest ice contents and vice versa. At these high values of θ_{ice}, not only have all voids been filled with ice, but the ice volume exceeds the porosity of dry silt. Consequently the samples with greater silt content have the higher values of ε' because of the unfrozen water between, or adsorbed on, the silt particles. If the value of θ_{ice} were to decrease below saturation, ε' would again decrease because air would continually replace water.

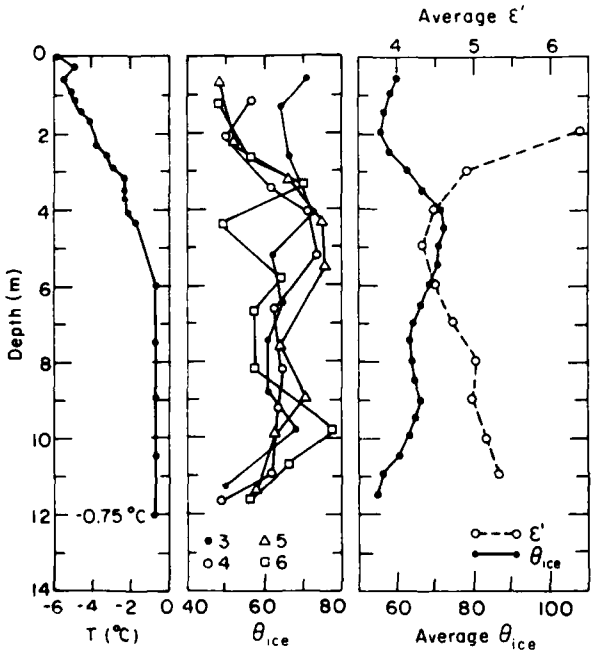

Figure 6. Temperature, individual volumetric ice content, and average dielectric constant and volumetric ice profiles (holes FL1–5).

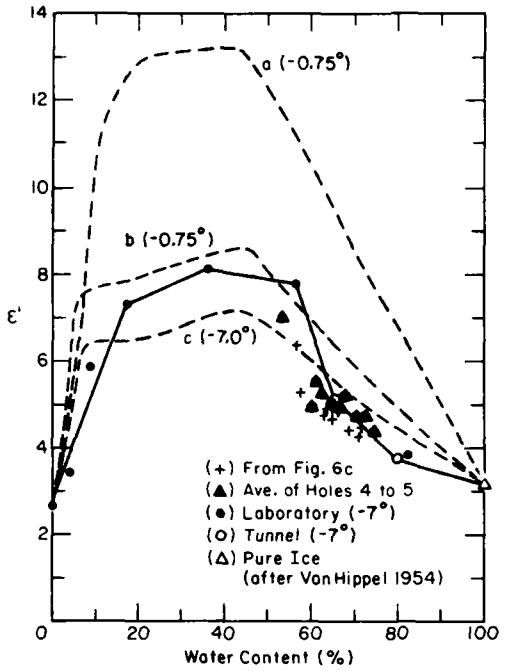

Figure 7. Dielectric constant vs volumetric water content data compared with previous investigations and theoretical results (dashed curves explained in text).

Consequently there is a nonlinear dependence of ε' on θ_{ice}.

This relationship is illustrated in Figure 7, which superimposes the dielectric data of Figure 6 (along with data for transmission from holes 4 to 5) on (revised) theoretical curves and other experimental data for frozen silt given by Delaney and Arcone (1984). The solid curve is based on both laboratory and field data taken at temperatures near –7°C. The crossed data points are the averages from Figure 6, and the dark triangles are the averages for just holes 4 and 5, both of which were sampled to calculate θ_{ice}. The dark triangles and the crosses agree well with the previous observations, although the temperature range for the borehole data was –0.75° to –6.0°C. This temperature insensitivity must be related to the only temperature-sensitive component, the unfrozen water, either through a significant reduction in the volumetric fraction of silt at high ice contents, or through a decrease in its own permittivity in the natural state.

The hypothesis that the temperature insensitivity is due to the reduced volumetric fraction of silt at high ice contents is tested by the theoretical curves in Figure 7, which are derived from

a simple volumetrically based dielectric mixing formula:

$$\varepsilon' = \sum_{m=1}^{4} \varepsilon'_m \theta_m . \qquad (7)$$

The index m is for ice, unfrozen water, air and dry silt. The ε' values of air, silt and ice are 1.0, 4.0 and 3.2, respectively; the dry sample porosity is 0.44; and the silt density is 2.7 g/cm^3. The unfrozen water is assigned an ε' of 84 at –0.75°C and 60 at –7.0°C (Stogryn and Desargent 1985), values that alter the previous version of this curve (Delaney and Arcone 1984) based on the value of $\varepsilon' = 88$. Curves b (–0.75°C) and c (–7.0°C) assume a capacity for unfrozen water of 4 g water/100 g silt, while curve a (–0.75°C) assumes a value of 8. Recent data from Tice et al. (in prep.), who used a nuclear magnetic resonance method, suggest that 8 (–0.75°C) and 4 (–4° to –7°C) are more appropriate. Thus, the wide separation of curves a and c near 60% water content means that, theoretically, the reduced amount of silt when the water (or ice) content is high is not sufficient to cause the temperature insensitivity that we observe from the data. An overestimate of ε' for supercooled unfrozen water does not seem possible in view of the high permittivities measured on well-mixed laboratory samples (Delaney and Arcone 1984). More-sophisticated models based on structural considerations would give a better match to the data, but they are not expected to alter the conclusion of a theoretical temperature sensitivity.

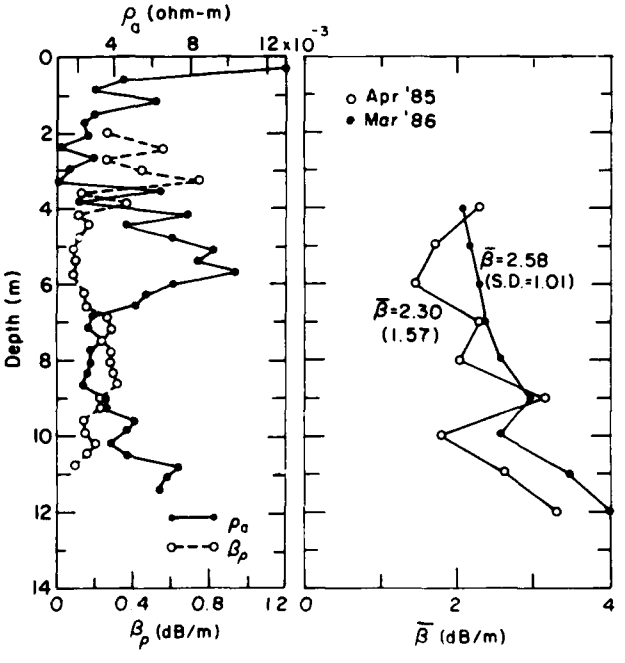

Figure 8. Resistivity (dc) and its associated signal attenuation rate, and average total attenuation rates for two years.

It seems, then, that the reduced temperature sensitivity is due to an inability of the silt to have reached its full capacity for retaining unfrozen water. It is unlikely that ice lens growth has occurred at the expense of the unfrozen water in the already frozen silt in view of the high degree of saturation and the NMR results of Tice et al. (in prep.). The possibility that not all silt particles ever came in contact with unfrozen water is also unlikely because this retransported section probably formed as an aggrading saturated active layer. Therefore, we can only speculate on the possibility of organics or molecular diffusion as agents of reduction in unfrozen water content.

Figure 8 shows resistivity vs depth. The values range from 1000 to over 12,000 ohm-m and are representative of silt to a radial distance of about 20 cm from the electrode string (Delaney et al. 1988). Also plotted are the equivalent attenuation rates β_ρ associated with these values. The lowest value (~1000 ohm-m) gives a maximum β_ρ of about 0.75 dB/m. Generally, however, most values below the 4-m depth are less than about 0.3 dB/m.

Figure 8 also shows the average propagation attenuation rate measured at each depth for April 1985 and March 1986. Average rates should compensate for variations caused by changes in antenna orientation (0.23 dB/m at most) or by dielectric inhomogeneities near the antennas. Ten to thirteen comparisons between borehole pairs were used to calculate each point. Averages above the 4-m depth are not given, either because of noise distortion or because too few signal levels could be read above the noise to give a meaningful average. The few values that could be calculated using borehole 6 are included in these averages. There is a general increase of attenuation with depth, which correlates with the increase in T and ε' with depth and the decreasing θ_{ice} values below 8 m. The minimum average value of 1.40 dB/m is well above the maximum rate of 0.75 dB/m due to conductive losses (Fig. 8). There is a general lack of dispersion in all waveforms (e.g. Fig. 5). This does not imply that dielectric relaxation or scattering (frequency-dependent processes) are not prevalent, because the ratio of bandwidth to center frequency (0.47) may be too small to allow dispersion to develop over these propagation distances. If scattering is the important loss mechanism, then the larger values of β

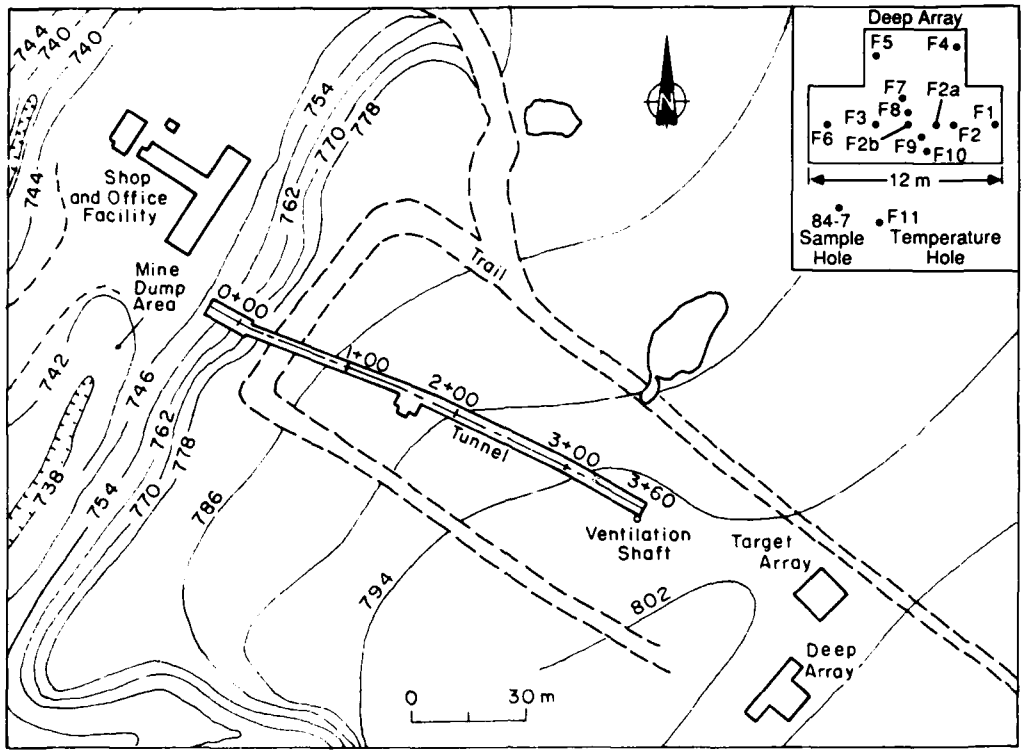

Figure 9. Location and borehole layout at Site 2 in Fox, Alaska, which contained massive ice. Contoured surface elevations and tunnel scale are in feet.

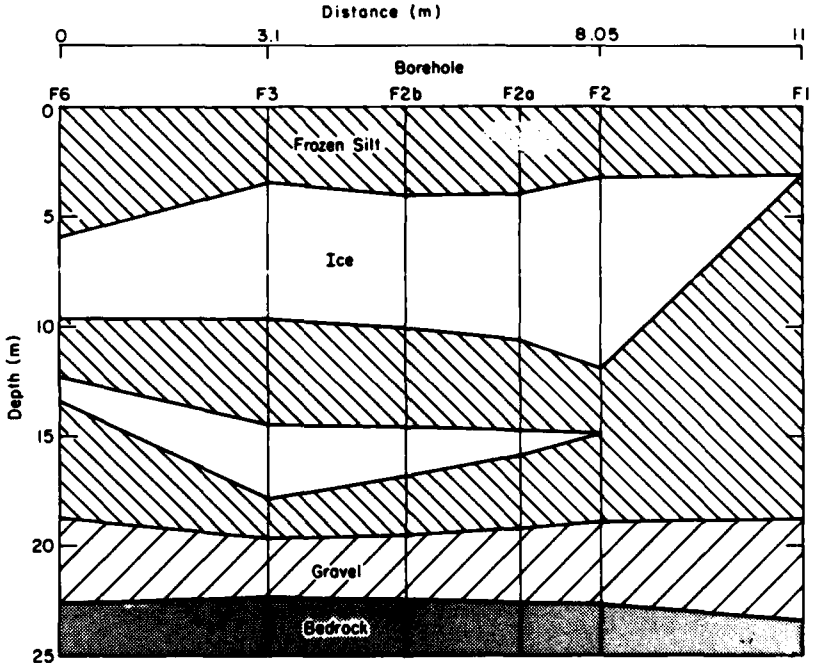

Figure 10. Well log interpretation for six holes at Fox, Alaska. (From Delaney 1987.)

below 8 m indicate greater inhomogeneity, as would the decrease in θ_{ice} from such high values at 4–6 m. The maximum value of 4 dB/m gives $n'' = 0.22$, which supplies an insignificant correction to the calculation of ε' as per eq 4.

Site 2: Massive ice

This site is located in perennially frozen ground near the CRREL permafrost tunnel at Fox, Alaska, on the margin of Goldstream Valley. It is situated on the lower slopes of a north-facing hillside. Fairbanks silt is the most abundant material in this area and was exposed in all of the holes. The geology and permafrost conditions have been extensively described by Sellmann (1967, 1972) and Péwé (1958).

Figure 9 shows the location and borehole layout of the area. It is accessible from the Steese Highway near Fox. The site contains two arrays spaced about 16 m apart. The target array was used for other purposes and is described by Delaney (1987), who also gave details of the drilling procedures and the hole logs. The deep array is the investigation site and consists of six holes (F1–F6) drilled to depths of 24 m (78 ft) through frozen silt and frozen gravel sections into the top of the bedrock (precambrian schist). An additional six uncased holes were drilled to further delineate the massive ice features encountered during the deep drilling.

Figure 10 shows the interpretation from the well logs for holes F1–F6. The top of the massive ground ice was encountered in several holes at depths between 3.4 and 4.6 m and was continuous to depths as great as 12.1 m. A second, deeper zone of massive ice was encountered in the 12.2- to 13.7-m depth range. Frozen gravels and bedrock were encountered beneath the frozen silt. Figure 11 shows the volumetric ice content determined from core samples taken from hole F7. Most of the values fall in the range seen at Site 1. Two of the values are higher than 90%, but the samples were not classifiable as massive ice.

Hole F11 was drilled to provide temperature data. The total depth was 18.3 m (to the top of the gravel). The hole was cased with 1.5-in. (3.8-cm) I.D. ABS pipe, which was filled with ethylene glycol. The remaining annulus was backfilled with drill cuttings and water. Figure 12 shows temperature profiles recorded throughout a nine-month period. The lowest ground temperature, –5.8°C, occurred at a depth of 1 m near the time of the transmission studies. The ground is permanently frozen at –0.76°C below 6.1 m.

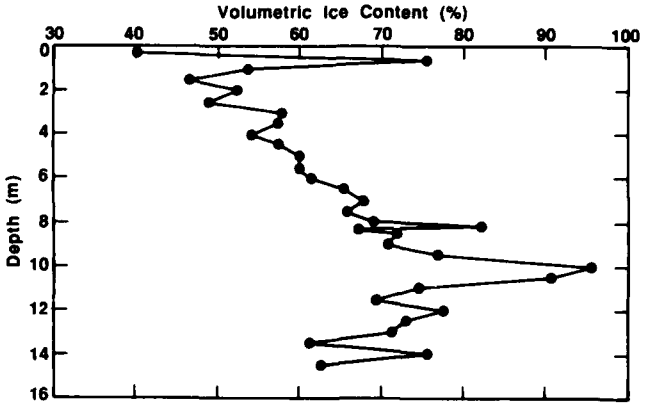

Figure 11. Volumetric ice content vs depth for samples from hole F7. (From Delaney 1987.)

Figure 13 shows the calculated dielectric constant as a function of depth, which can then be compared with the well log interpretations of Figure 10. There is a good correlation between the low values of ε' and the section of massive ice between holes F2 and F3. Here, between 4 and 10 m, ε' ranges from 2.9 to 3.6 for both March and September. In the central part of the massive ice between 6 and 9 m, ε' ranges between 3.1 and 3.3;

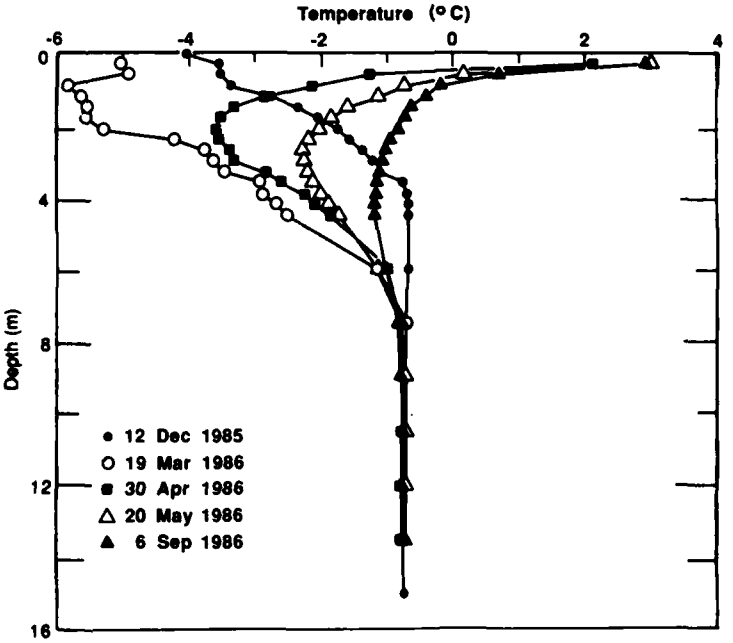

Figure 12. Vertical temperature profiles recorded in hole F11. (From Delaney 1987.)

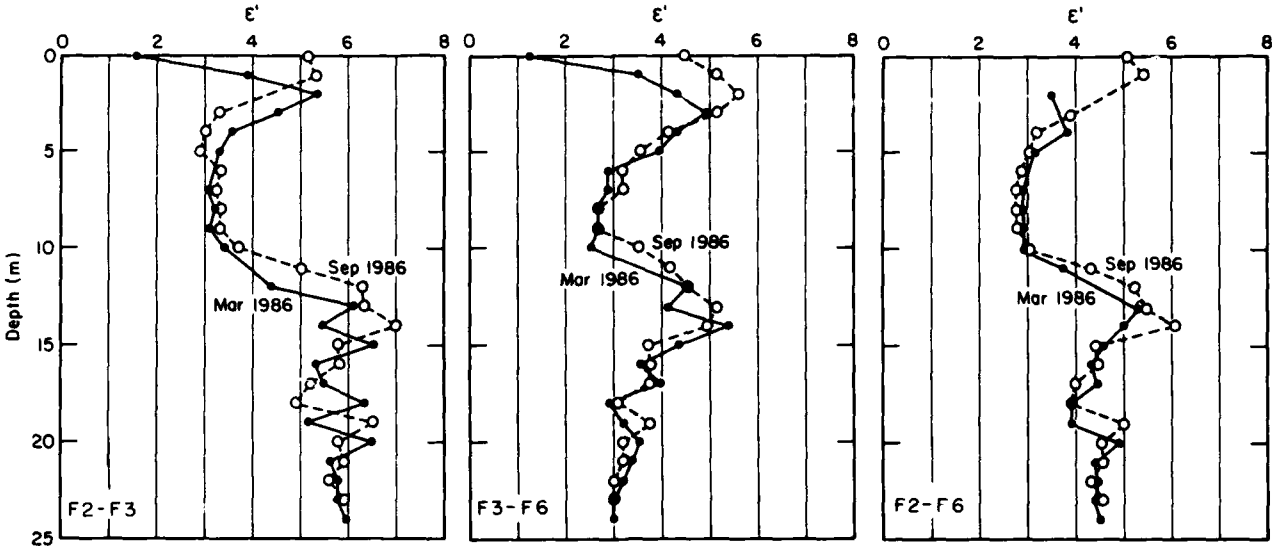

Figure 13. Dielectric constant vs depth at two times of year for three of the borehole pairs shown in Figure 10.

ε' for pure ice is 3.2. Between 10 and 15 m deep, ε' increases to between 4 and 7 for the section of frozen silt, the same range as at the Farmers Loop site. Below 15 m there are at least three transitions in material type, and the ε' values vary between 5 and 6.5 before apparently steadying at about 5.8 in the bedrock. In these lower regions the dominant in-situ wavelength ranges between 1.2 ($\varepsilon' = 6.5$) and 1.3 m ($\varepsilon' = 5.0$), so that the lower layers of either ice, silt, gravel or bedrock are generally about 2–3 wavelengths thick. This can cause waveguiding, which would increase the apparent value of ε' by slowing the energy propagation velocity due to reflections along the waveguide boundaries.

The results for propagation between holes F3 and F6 (Fig. 13) differ from those for holes F2–F3. There is a more gradual transition to the low values in the massive ice section, probably because of the tapered upper boundary suggested by the well logs. Within the massive ice, ε' ranges between 2.5 and 3.2, values that have been observed previously (Annan and Davis 1976). Annan (1976) thought that these low values were caused by air bubbles, but this was not borne out by our core samples, although highly porous ice has been observed elsewhere in the area.* The ε' values again increase into the frozen silt, but in this case only as high as 5.5. Then, below 15 m, ε' drops to as low as 3 in the bedrock. This low value is most likely due to a loss of water content severe enough to preclude adsorption on the grain surfaces.

The results of propagation from F2–F6 (Fig. 13) again show low ε' values in the upper massive ice formation, varying values from 10 to 20 m, and finally a steady value of about 4.5 in the bedrock. Figure 14 then shows the percentage difference between the travel times of F2–F6 and those from the combined results of F2–F3 and F3–F6. In most cases the difference is under 10%, with over half the depths giving differences of

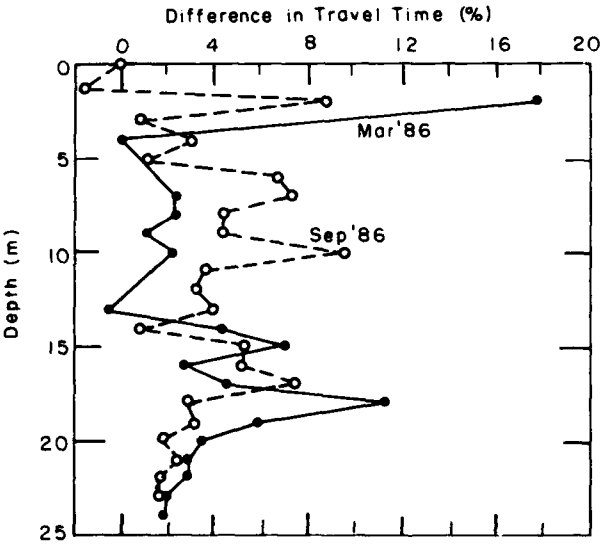

Figure 14. Percent difference in travel time between propagation from F2–F6 and the combined times of F2–F3 and F3–F6.

* Personal communication with D. Lawson, CRREL.

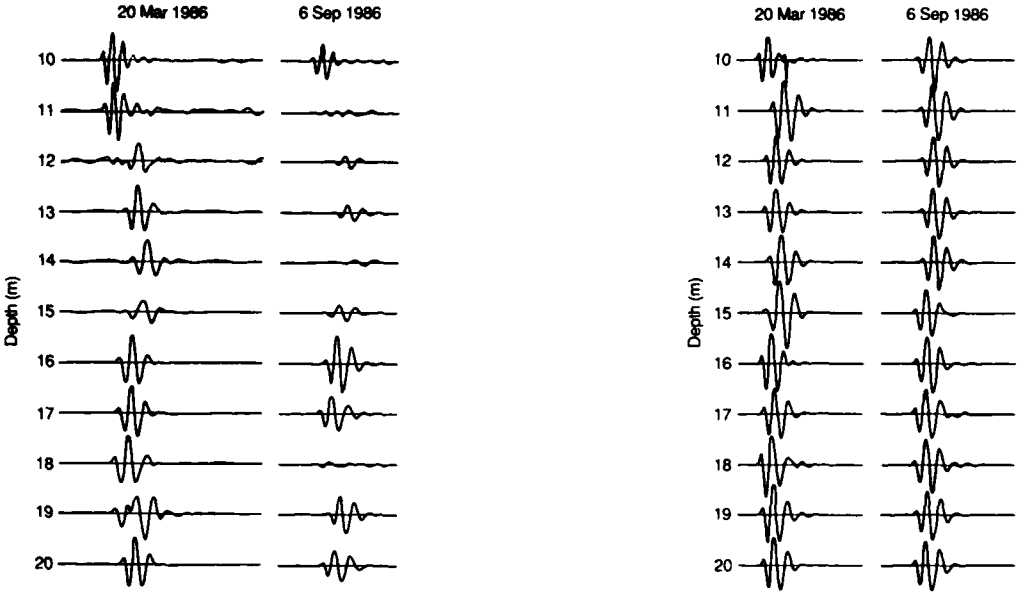

a. Waveforms transmitted between holes F2 and F6 (805 cm).

b. Waveforms transmitted between holes F3 and F6 (310 cm).

Figure 15. Seasonal comparison of waveforms. Variations in waveform between seasons are probably due to differences in propagation paths, as antenna placement could not be accurately reproduced at the later date. The closer spacing between F3 and F6 gives greater consistency between seasons.

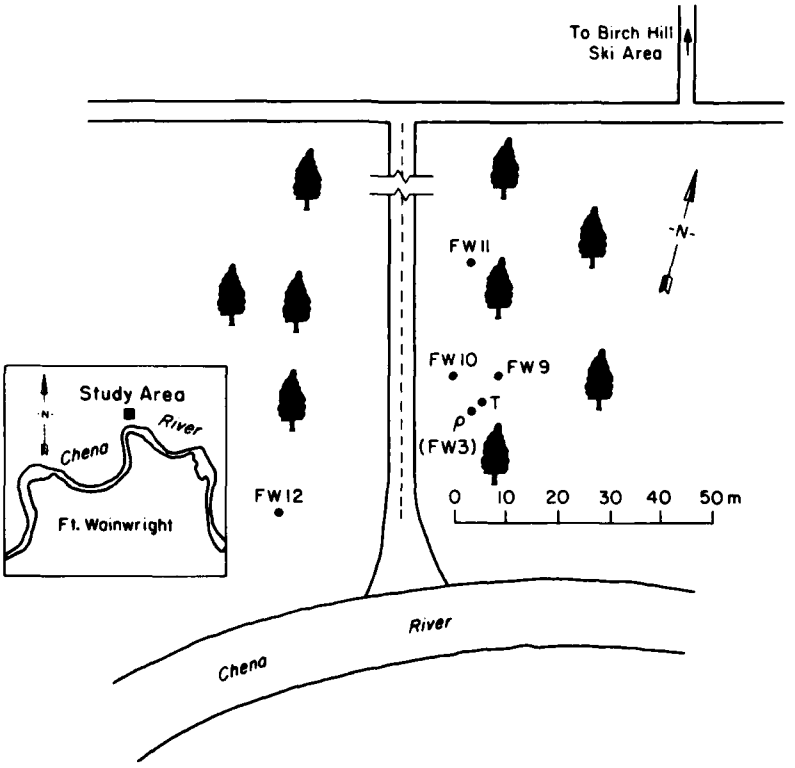

Figure 16. Location and borehole placement for Site 3 on Ft. Wainwright, which contained frozen alluvium.

less than 4%. The differences are less than 2% at the lowest depths, presumably reflecting the homogeneity of the bedrock beneath 23 m. All but two points in the figure are positive differences, meaning that the combined times for the two separate paths are generally greater than those of the single path. This consistency in sign is believed to be a source-related problem at F3, because the path of least time between F2 and F6 may not necessarily pass through F3.

The temperature curves of Figure 12 show the ground to be frozen below a depth of 1 m for September and to have the same temperature profile below 6 m for both March and September. Therefore, the variation in ε' values between seasons beneath 6 m is probably due to inaccuracies in antenna repositioning (estimated at ±0.25 m) about the several material transitions. This explanation is strengthened by the variations in amplitude and waveshape between seasons (Fig. 15). Waveguide modes within layers can cause waveform distortion, and the excitation of such modes can easily depend on the position of an antenna phase center relative to a material interface.

Site 3: Frozen alluvium

This site is located near the Chena River on Ft. Wainwright in an area mapped as flood-plain sand and gravel (Péwé 1958). The annual active layer thickness is usually about 1.5 m, and the soils are continuously frozen to at least 12.2 m, the depth of the four 8-in.-diameter (20.3-cm) cased holes used for cross-borehole transmission. The layout of these holes and the resistivity electrode string and temperature holes is shown in Figure 16.

Figure 17 summarizes the gravimetric analyses for hole FW12 and compares them with values of ε' determined from propagation between holes FW10–12, a distance of 42.97 m. The gravimetric percentages of silt, sand and gravel were determined after the water and organics were removed and are not adjusted for the original water and organic content. The finest mesh size

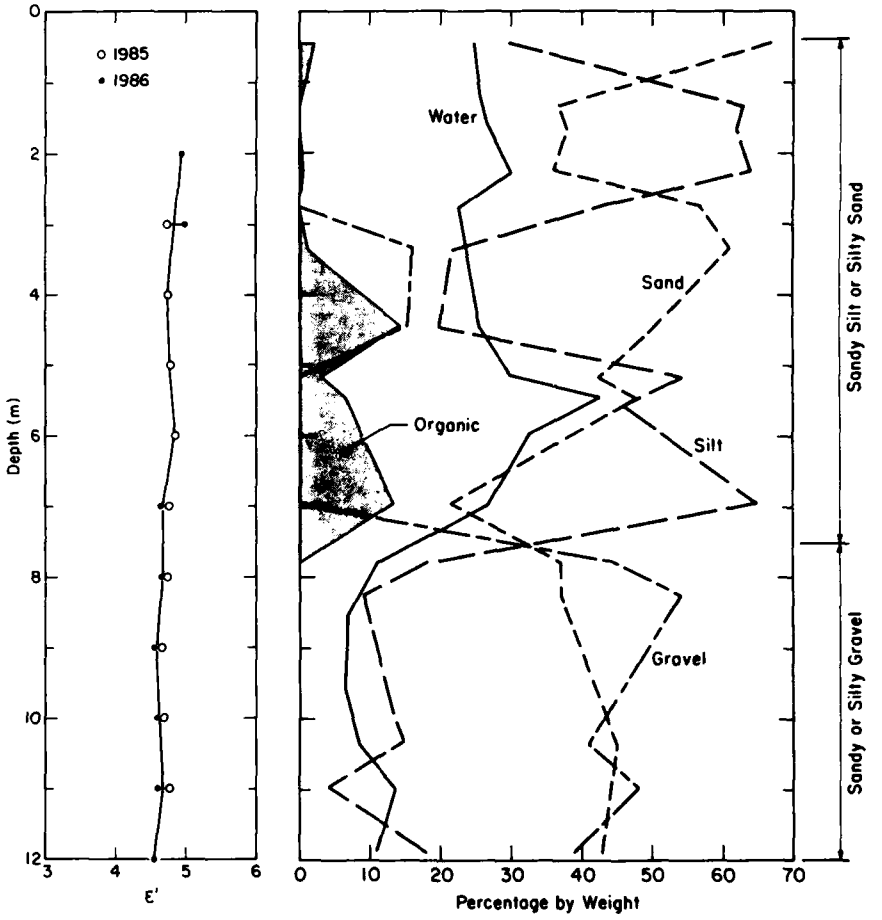

Figure 17. Comparison between the dielectric constant measured for FW10-12 propagation and gravimetric soil analysis of hole FW12. The percentages of silt, sand and gravel are of the dried weight after ignition of all organics.

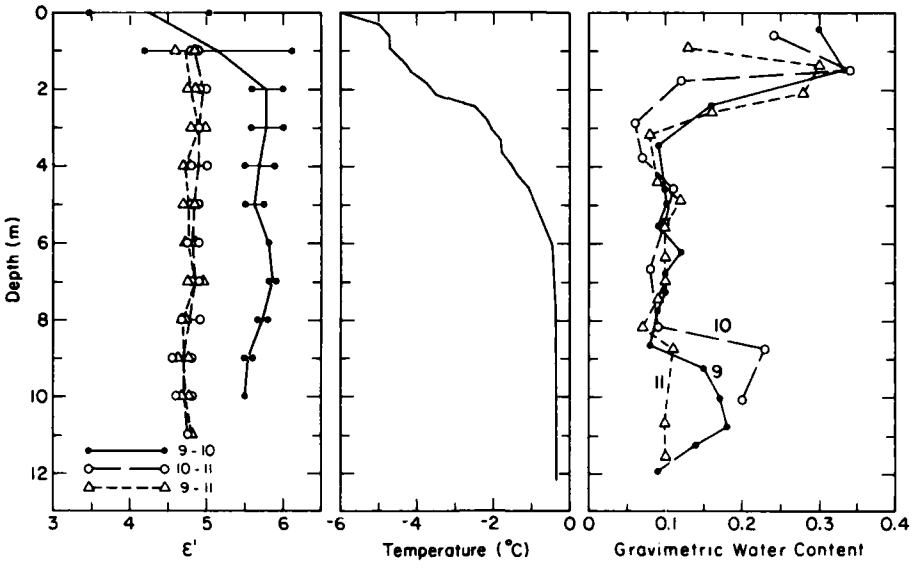

Figure 18. Dielectric constant vs depth for all three hole pairs for 1984–1986 compared with temperature and gravimetric water content.

was 0.074 mm, and all grains passing this size were classified as silt. Grains not passing a mesh size of 4.76 mm were classified as gravel. For the gravelly samples, grain sizes exceeding 20 mm in diameter were less than 10% by weight, and no grain sizes exceeding 40 mm were retained.

The only variation apparent in Figure 17 is a slight decrease of ε' with depth. From 0 to 6 m in depth the average ε' varies between 4.75 and 4.95 (±0.03), while below 6 m it varies between 4.55 and 4.68. This correlates with a large decrease in silt content (between 7 and 8 m) and in gravimetric water content (between 6 and 8 m). It is therefore hypothesized that the slight variation of ε' can be explained by the slight decrease of adsorbed water (which exists primarily on the silt) with depth. For example, a 100-g sample at a depth of 2 m has a water content of 29 g, a silt content of 0.64 (100–29) = 45 g, and a sand content of 26 g. Near a depth of 12 m the water content is 11 g, the silt content is 16 g, the sand content is 38 g and the gravel content is 35 g. Assuming the silt surface area to be the only significant contributor to unfrozen water content, and extrapolating the data of Tice et al. (1978), we estimate that there is approximately 1.4 g of unfrozen water (0.03 g/g silt at 29% water content) and 27.6 g of ice at a depth of 2 m (T = 3.5°C; see below), and 0.6 g of unfrozen water (0.04 g/g silt at 11% water content) and 10.4 g of ice near the depth of 12 m (T = –0.35°C) in hole FW12. Given similar porosities at both depths, and an ε' for adsorbed water of 75 at –3.5° and 85 at 0.35°C (Stogryn and Desargent 1985), the dielectric contribution of the adsorbed water is 75 x 0.014 = 1.05 at 2 m and 85 x 0.006 = 0.5 at 12 m, assuming a simple volumetrically based dielectric mixing formula (eq 7). This results in an ε' difference of about 0.5 for the two depths and compares favorably with the maximum measured difference of 0.4 between values above and below 6 m. In addition to the above assumptions, it must also be considered that each of the dielectric measurements represents an integration through 43 m of soil. However, ε' and grain data presented below show the geology of the area to be fairly uniform.

Figure 18 gives the ε' profiles for propagation between FW9–10, 9–11 and 10–11 for early spring 1984–1986, along with the temperature and gravimetric water profiles. The uniformity of the ε' profiles shows that the variation in temperature and water content have little effect on ε', as was shown above. The ε' profiles for FW10–11 and 9–11 are almost identical to those in Figure 17. The exception is the ε' profile for propagation between FW9–10, where ε' values range between 5.5 and 6.0 at 2 m and deeper (values for depths nearer the surface may have been influenced by refraction along the air/soil boundary). These deviations are probably due to a local increase in water content, but how this can be effected is not known. Gravimetric analyses of the soil samples from four holes for two depth zones (Fig. 19) show the general uniformity of soil stratification throughout the study area.

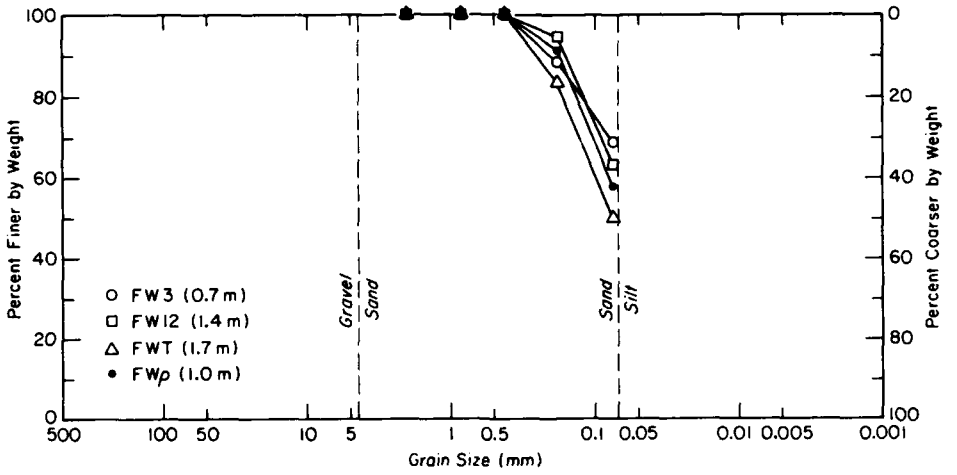

a. 0.7–1.7 m deep.

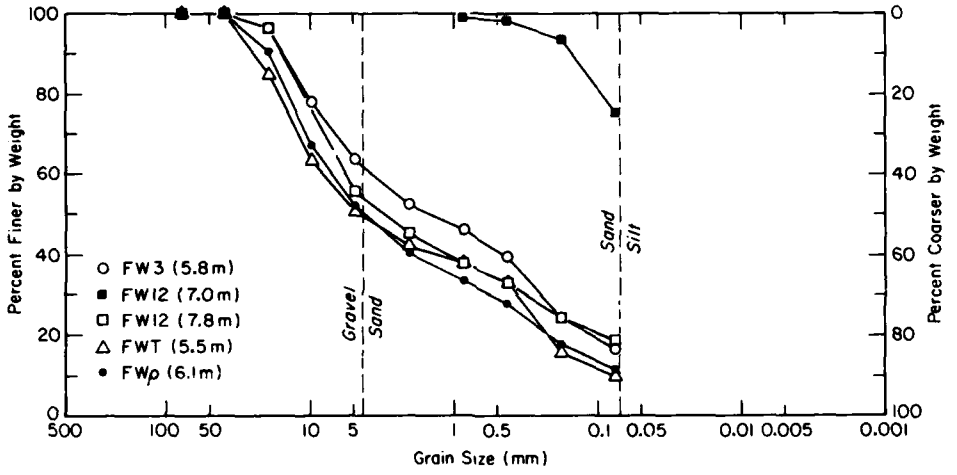

b. 5.5–7.8 m deep.

Figure 19. Grain size distribution in four holes at two depths. Hole FW12 shows a transition to the coarser texture just below the 7-m depth.

Figure 20 compares the measured attenuation rate β with β_ρ, the rate due only to conductive absorption processes. The quantity β_ρ is derived from dc apparent resistivity data taken on 4 April 1986. As explained previously, the values are corrected for losses due to geometric spreading; the reference hole pair was FW9–10. The ranges given for the β values at each depth cover the years 1984–1986. The dashed and solid continuous lines connect the average values of β. The calculated values were expected to be consistent between years but rarely were, as suggested by the wide ranges seen about the averages, so the accuracy of the amplitude measurement is questionable. For all readings of FW10–11, $\bar{\beta} = 0.72$ (S.D. = 0.50), and for FW 9–11, $\bar{\beta} = 0.62$ (S.D. = 0.37). Below 1 m the maximum value of β_ρ at any depth never exceeds the maximum value of β at the same depth. Therefore, conductive absorption never accounts for all of the propagation attenuation beyond geometric spreading. Generally, β is very low in comparison with the silt values measured at Farmers Loop. Below 6 m, where the silt content becomes very small (Fig. 19), the apparent resistivity steadies at around 10^4 ohm-m and β_ρ is generally less than 0.1.

The lack of variation in dielectric properties of the rock material, coupled with the large size of the in-situ wavelength (137 cm at 100 MHz) in comparison with the grain sizes, leads to the con-

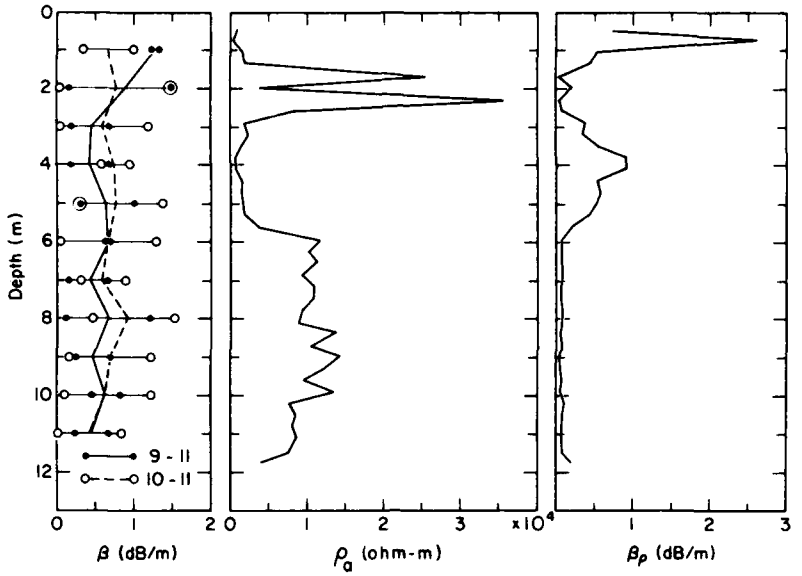

Figure 20. Attenuation rate β for two hole pairs vs depth compared with dc apparent resistivity and equivalent resistive attenuation rate β_ρ. Ranges for the β values at each depth cover the years 1984–1986. Dashed and solid continuous lines for β connect average values.

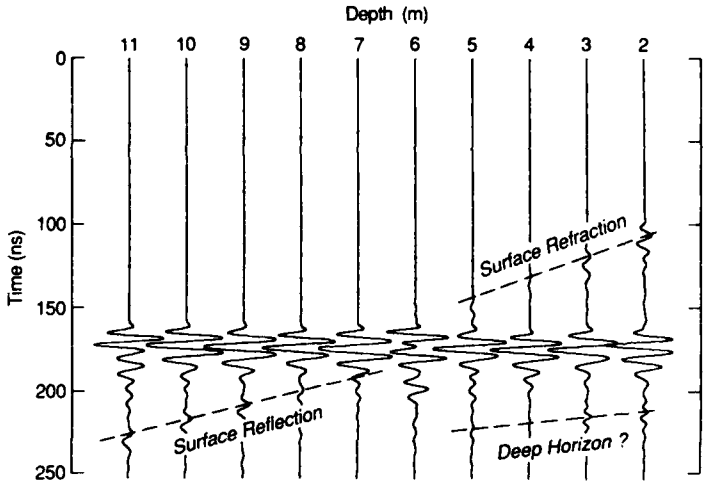

Figure 21. Transmission record for hole pair FW10–11, revealing four events, three of which can be seen in the 2- and 3-m traces.

clusion that losses due to scattering from individual grains are also negligible. In addition, at a 20-m separation the maximum antenna directional gain loss of 2.6 dB translates to only 0.13 dB/m, so the measured β values of 0.05–1.5 dB/m cannot be due to the different rotational positions of the antennas in the borehole (discussed above). The one remaining explanation for the measured range of β is scattering losses from uneven distributions of unfrozen or adsorbed water (mainly associated with the silt), the weight percentage of which can quadruple over the distance of just a few meters (Fig. 17). The variations of β at any one depth from year to year are most likely due to inexact repetition of the vertical antenna position within the boreholes.

These calculations of ε' and β all presumed straight-line propagation between boreholes. Since the ε' profiles show little variation, there is no reason to believe that this is not the case. The data, however, do reveal that other propagation paths between all hole pairs did occur. These other paths can be seen in Figure 21, which gives all traces for April 1986 for the pair FW10–11; the amplitude of two of these traces is enlarged in Figure 22. In Figure 21 there are three arrivals apparent at the 2- and 3-m depths and two arrivals apparent at all other depths. The strongest arrival is the direct transmission. One series of events in Figure 21 is marked "surface refraction." The latest event occurring in the top three traces in Figure 21 comes from an unknown horizon within the alluvium and may have arrived too late to be recorded below the 3-m depth. The latest arrivals in the bottom four traces are believed to be a surface reflection, which inter-

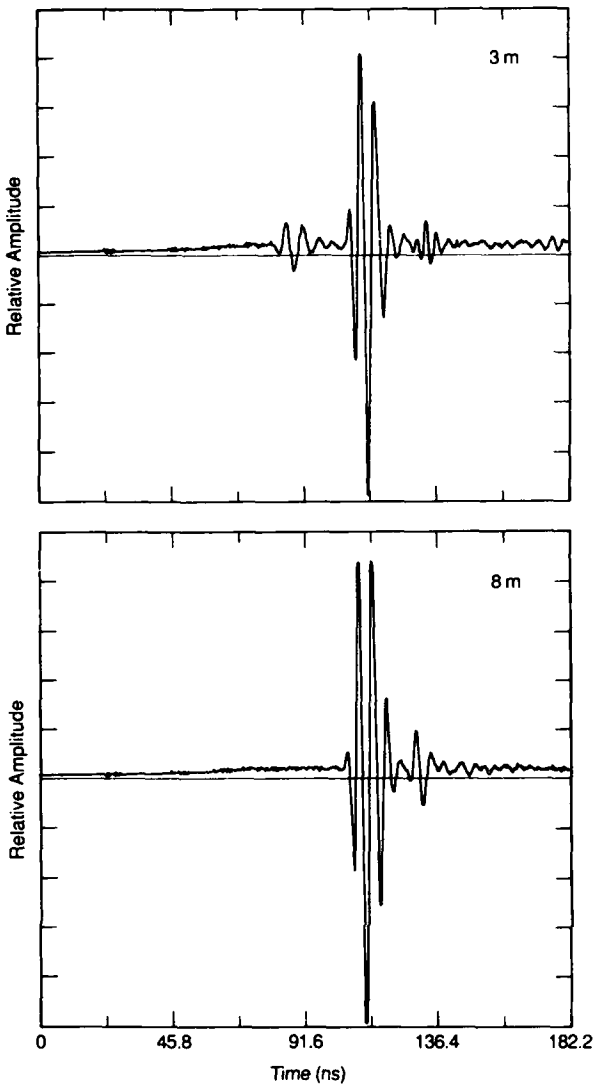

Figure 22. Amplitude enlargement of the 3- and 8-m traces of Figure 21.

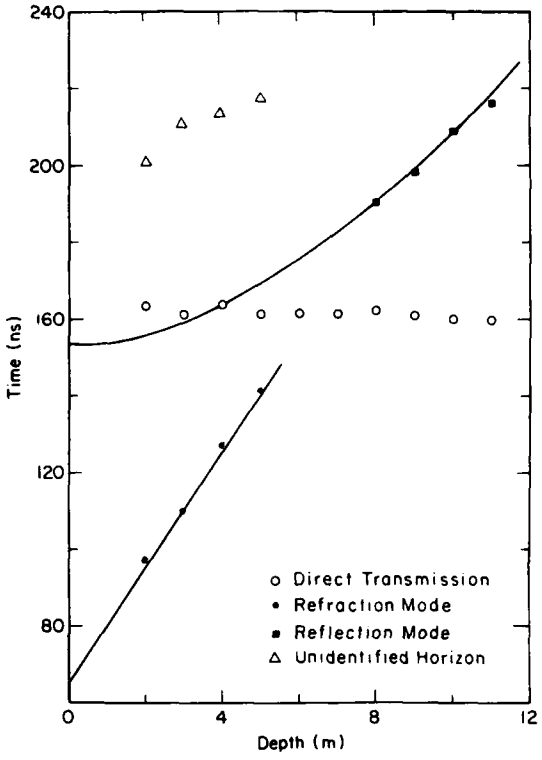

a. Time vs depth plot of the leading edge of the four events.

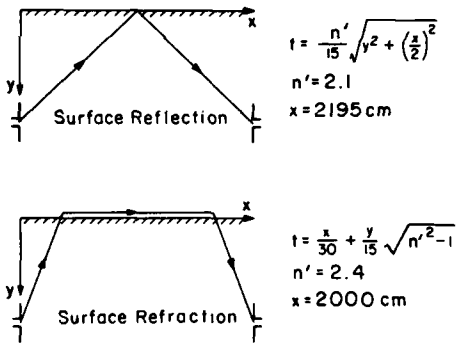

b. Models that fit two of the events in a: surface reflection model and surface refraction model.

Figure 23. Four events from Figure 21 for propagation between FW10–11.

feres with the direct transmission at the 6- and 7-m depths.

Figure 23 shows the arrival time vs the antenna depth for the four events in Figure 21. Two models are proposed in Figure 23 for interpreting the indirect transmissions. The best fit to the earliest event between 2 and 5 m is achieved with a surface refraction model (also known as an up-over-down mode) using a borehole separation of 2000 cm and an n' value of 2.40. This compares fairly well with the average n' of 2.20 computed from the direct transmissions and the actual separation of 2195 cm. The model of a direct reflection from the surface using $n' = 2.10$ gives time delays that best fit the arrival times of the later events at the deepest depths. The interference apparent in Figure 21 at the 6-m depth is probably due to the superposition of the direct transmission and surface reflections. The third event in Figure 21 at 2- and 3-m depths (plotted as open triangles in Fig. 23) is believed to be a direct reflection from a more distant, but not necessarily deeper, horizon.

SUMMARY AND CONCLUSIONS

Cross-borehole pulse propagation can be an effective means of generally assessing the volumetric ice content in frozen silt. Although ε' does not seem to be sensitive to temperature in the cases studied, such sensitivity could exist in other silt deposits depending, probably, on lithologic or historical factors not now understood. The nonlinear dependence of ε' on θ_{ice} requires, however, other information to establish if θ_{ice} is greater or less than about 40%. This can be done easily with a noncontact surface or borehole resistivity technique such as double dipole magnetic induction (e.g., Arcone et al. 1978). Values above 1000 ohm-m generally indicate that $\theta_{ice} >$ 40%. It is not at all clear that propagation attenuation rates could be used to diagnose the range of θ_{ice}, because increasing losses due to decreasing resistivity may be compensated for by less scattering due to increased homogeneity. The overall average of 2.3–2.6 dB/m found at the Farmers Loop site means that borehole separations greater than 20 m will need more power or increased dynamic range for this technique to assess the ice content of frozen silt.

The investigations conducted at the Fox site showed that sections of massive ice contrast in dielectric constant with many materials common to interior Alaska. However, the dielectric constants measured both at this site for ice-rich frozen silt, frozen gravel and frozen bedrock, and at the Fort Wainwright site for frozen alluvium, all fell within a similar, narrow range of values. Therefore, in areas where the material type is not known, cross-borehole propagation can at best indicate only zones of stratigraphic changes and of massive ice.

There are several positive aspects to the alluvial investigations at Fort Wainwright. The first is that propagation beyond 30 m (100 ft, a commonly used spacing in site investigations) is easily achieved. Second, there is great dielectric homogeneity over a variety of grain size distributions, with silt being the only component to which ε' may be sensitive. This is logical because silt in a fluvial environment is sure to retain some unfrozen water. Third, propagation occurred over distinct, recognizable paths. Therefore, the interpretation will not be affected by appreciable raypath curvature due to gradients in the refractive index. Fourth, transmitted waveforms did not undergo any significant dispersion. This is expected in a conductive-type low-loss medium or where losses are due to scattering. The frozen silt must still be considered a nondispersive medium despite the higher attenuation rate.

LITERATURE CITED

Annan, A. P. (1976) Density of ice samples from "Involuted Hill" test site, District of Mackenzie. Report of Activities, Geologic Survey of Canada, Paper 76-1C, Part C, p. 91–95.

Annan, A. P. and J. L. Davis (1976) Impulse radar sounding in permafrost. *Radio Science,* 11(4): 383–394.

Arcone, S. (1984a) Field observations of electromagnetic pulse propagation in dielectric slabs. *Geophysics,* 49(10): 1763–1773.

Arcone, S. (1984b) Pulse transmission through frozen silt. USA Cold Regions Research and Engineering Laboratory, CRREL Report 84-17.

Arcone, S. A. and A. J. Delaney (1982) Dielectric properties of thawed active layers overlying permafrost using radar at VHF. *Radio Science,* 17(3): 618–626.

Arcone, S. A. and A. J. Delaney (1984) Field dielectric measurements of frozen silt using VHF pulses. *Cold Regions Science and Technology,* 9: 29–37.

Arcone, S. A. and A. J. Delaney (1988) Borehole investigations of the electrical properties of frozen silt. *Proceedings, Fifth International Conference on Permafrost, Trondheim, Norway,* vol. 2, p. 910–915.

Arcone, S. A., P. V. Sellmann and A. J. Delaney (1978) Shallow electromagnetic geophysical investigations of permafrost. *Proceedings, Third International Conference on Permafrost, Edmonton, Alberta,* vol. 1, p. 501–507.

Barringer, A. R. (1965) Research directed to the determination of subsurface terrain properties and ice thickness by pulsed VHF propagation. Air Force Cambridge Research Laboratories, Report AFCRL-64-936, Barringer Research Ltd., Toronto, Canada.

Cook, J. C. (1960) Proposed monocycle pulse VHF radar for airborne ice and snow measurements. AIEE, Transaction Paper 60-994.

Davis, J. L., W. J. Scott, R. M. Morey and A. P. Annan (1976) Impulse radar experiments on permafrost near Tuktoyaktuk, N.W.T. *Canadian Journal of Earth Sciences,* 13: 1584–1590.

Delaney, A. J. (1987) Preparation and description of a research geophysical borehole site containing massive ground ice near Fairbanks, Alaska. USA Cold Regions Research and Engineering Laboratory, Special Report 87-7.

Delaney, A. J. and S. A. Arcone (1984) Dielectric measurements of frozen silt using time domain reflectometry. *Cold Regions Science and Technology,* 9: 39–46.

Delaney, A. J., P. V. Sellmann and S. A. Arcone (1988) Seasonal variations in resistivity and temperature in discontinuous permafrost near Fairbanks, Alaska. *Proceedings, Fifth International Conference on Permafrost, Trondheim, Norway,* vol. 2, p. 927–932.

Hoekstra, P. and A. J. Delaney (1974) Dielectric properties of soils at UHF and microwave frequencies. *Journal of Geophysical Research,* 75(11): 1699–1708.

Morey, R. M. (1974) Continuous subsurface profiling by impulse radar. *Proceedings of Engineering Foundation Conference on Subsurface Exploration for Underground Excavation and Heavy Construction, 11–16 August 1974, Henniker, N.H.* Published by American Society of Civil Engineering, New York, p. 213–232.

Péwé, T. L. (1958) Geology of the Fairbanks (D-2) Quadrangle, Alaska. U.S. Geological Survey, geological quadrangle map GQ-110.

Sellmann, P. V. (1967) Geology of the USA-CRREL permafrost tunnel, Fairbanks, Alaska. USA Cold Regions Research and Engineering Laboratory, Technical Report 199.

Sellmann, P. V. (1972) Geology and properties of materials exposed in the USACRREL permafrost tunnel. USA Cold Regions Research and Engineering Laboratory, Special Report 177.

Sellmann, P. V., S. A. Arcone and A. J. Delaney (1983) Radar profiling of buried reflectors and the groundwater table. USA Cold Regions Research and Engineering Laboratory, CRREL Report 83-11.

Stogryn, A. and G. Desargent (1985) The dielectric properties of brine in sea ice at microwave frequencies. *IEEE Transactions on Antennas and Propagation,* AP-33(5): 40–48.

Tice, A. R., C. M. Burrous and D. M. Anderson (1978) Phase composition measurements on soils at very high water contents by the pulsed nuclear magnetic resonance technique. In *Moisture and Frost-Related Soil Properties,* Transportation Research Board, National Academy of Sciences.

Tice, A. R., P. Black and R. Berg (in prep.) Unfrozen water contents measurements of undisturbed and remolded soils from the Northwest Alaska Pipeline Company frost heave facility as determined by pulsed nuclear magnetic resonance. USA Cold Regions Research and Engineering Laboratory, CRREL Report.

Von Hippel, A. R. (Ed.) (1954) *Dielectric materials and applications.* New York: John Wiley Sons, Inc.

A facsimile catalog card in Library of Congress MARC format is reproduced below.

Arcone, Steven A.

Investigations of dielectric properties of some frozen materials using cross-borehole radiowave pulse transmissions / by Steven A. Arcone and Allan J. Delaney. Hanover, N.H.: U.S. Army Cold Regions Research and Engineering Laboratory; Springfield, Va.: available from National Technical Information Service, 1989.

iv, 26 p., illus., 28 cm. (CRREL Report 89-4.)

Bibliography: p. 17.

1. Alaska. 2. Dielectric properties. 3. Frozen soils. 4. Radiowaves. 5. Site surveys. I. Delaney, Allan J. II. United States Army. III. Corps of Engineers. IV. Cold Regions Research and Engineering Laboratory. V. Series: CRREL Report 89-4.

☆ U. S. GOVERNMENT PRINTING OFFICE: 1989--600-057--82085